

Note

Precise Lamb-dip measurements of millimeter and submillimeter wave rotational transitions of $^{16}\text{O}^{12}\text{C}^{32}\text{S}$

G.Yu. Golubiatnikov^{a,*}, A.V. Lapinov^a, A. Guarnieri^{b,c}, R. Knöchel^b

^a Institute of Applied Physics of the Russian Academy of Sciences, 46 Uljanova Street, GSP-120, 603950 Nizhnii Novgorod, Russia

^b Technische Fakultät der Christian-Albrechts-Universität zu Kiel, Lehrstuhl für Hochfrequenztechnik, Kaiserstraße 2, Kiel D-24143, Germany

^c Institut für Physikalische Chemie der Christian-Albrecht-Universität zu Kiel, Ludewig-Meyn-Street 8, 24118 Kiel, Germany

Received 6 June 2005; in revised form 17 August 2005

Available online 17 October 2005

The high precision laboratory spectra of molecules in millimeter- and submillimeter-wave ranges with uncertainties ≤ 1 kHz are in great demand nowadays for astrophysical studies [1,2]. To improve the performance of the submillimeter BWO-based spectrometer at the Technische Fakultät der Universität zu Kiel for such measurements, the Lamb-dip absorption technique has been used to identify the centers of spectral lines. To check our accuracy we select the $^{16}\text{O}^{12}\text{C}^{32}\text{S}$ molecule, which is a very stable chemical compound with simple rotational spectrum, not affected by any perturbation interaction in the ground vibrational state. The relatively strong dipole moment of 0.715 D [3] and the quite high density spectrum (12-GHz line spacing) make the OCS molecule one of the most used in laboratory test measurements. From the astrophysical point of view OCS, being one of the most common sulphur-bearing species, represents significant interest and is used as a density probe towards many warm and cold interstellar clouds and even for gas in other nearby galaxies (see [4,5] and references therein).

Rotational transitions of $^{16}\text{O}^{12}\text{C}^{32}\text{S}$ in the ground vibrational state were measured by many authors mostly below 200 GHz, and a very high accuracy was achieved in early Lamb-dip [6,7] and molecular beam [8–11] experiments. De Vreede et al. [12] could not find out any noticeable pressure induced line shift at room temperature for the OCS $J = 3 \leftarrow 2$ transition within an accuracy of 6 kHz/Torr; this feature was another important argument to select the molecule for our studies. The line center determined in [12] was consistent with a previous Lamb-dip measurement by

Costain [6], the discrepancy of 0.7 kHz is within experimental uncertainty.

Our measurements above 200 GHz have shown discrepancies with the Lamb-dip frequencies given by Winton and Gordy [7] which are systematically shifted in the order of +5 kHz. Further there are also no sufficiently precise data available at submillimeter frequency range. To eliminate this gap, Lamb-dip measurements of all rotational transitions of $^{16}\text{O}^{12}\text{C}^{32}\text{S}$ in the vibrational ground state were carried out for the frequency range 200–490 GHz. The OCS $J = 4 \leftarrow 3$ and $J = 7 \leftarrow 6$ transitions have been measured to test the spectrometer precision in mm-frequency range, and this was necessary for our studies of other molecular species, and because of the lack of accurate data at 85 GHz frequency. Supplementary measurements by conventional line absorption technique of OCS lines by 922 and 934 GHz were also performed for the same reason. To make our data more reliable, additional measurements in THz range were also performed by another method using a spectrometer with radio-acoustic detection (RAD) in the microwave laboratory of Nizhnii Novgorod.

Millimeter and submillimeter waves in the frequency range 200–500 GHz were obtained directly from the BWO (backward wave oscillator) tubes OB-30 and OB-32 manufactured by ISTOK (Russia). The tubes were phase-stabilized against a 75–110 GHz source (sextupler HP 83558A), driven by the frequency synthesizer HP 8673G (2–26 GHz) provided with an amplifier (HP 8349B). A computer controlled PTS 500 synthesizer was used as fast frequency sweeper in the 35 MHz reference channel of the BWO synchronizer. The synthesizers were stabilized against a 10 MHz Meinberg GPS 166 Satellite controlled clock having a frequency stability $\Delta f/f$ of $\sim 10^{-9}$ (for some description of the Kiel spectrometer see Ref. [13]). The

* Corresponding author. Fax: +8312 36 3792.

E-mail addresses: glb@appl.sci-nnov.ru (G.Yu. Golubiatnikov), ag@tf.uni-kiel.de (A. Guarnieri).

Lamb-dip geometry of the spectrometer includes a wire grid polarizer at one side of the gas cell (length 4.2 m, diameter 10 cm) and a roof top reflector at the other side to get two waves propagating in opposite directions. The wire grid polarizer led the radiation to an InSb-bolometer cooled down to 4.2 K by means of a Quantum Technology closed cycle cooling device. The InSb chip was of the type QFI/X delivered by QMC Instruments (UK). Frequency and phase modulations with second harmonic detection were employed by the measurements with modulation rate of 2–5 kHz and frequency deviation depth of 10–40 kHz.

For the measurements in the THz range the tube ISTOK OB-83 was used in the frequency range 900–1100 GHz with phase-stabilization through two locked loops, the first of which with a klystron VRE-2103B (Varian, Canada). For some reasons, only two OCS lines and one CO line in 900 GHz range were measured with the spectrometer at the Kiel University.

Frequencies of 12 OCS lines and 2 CO lines were measured in the THz range by the RAD spectrometer at Nizhnii Novgorod. These measurements were carried out at a

pressure of 0.1–0.3 Torr (the pressure and Doppler broadenings were of the same order of magnitude) by means of amplitude modulation (description of RAD spectrometer is given in [14]). All studies in Kiel and in Nizhnii Novgorod were performed at the room temperature of 300 ± 1 K.

The observed frequencies for all transitions were obtained as averages of many line records (usually between 10 and 20) at slightly different experimental conditions, e.g., line position on the baseline. Line centers were determined by a line-profile fitting program which uses Fortran codes developed by us and similar to that described in [15,16] but improved for the use at any power saturation. An example of measured line shape is shown in Fig. 1. The main source for the line position uncertainty is due to some systematic shift caused by interference between the molecular line and the baseline signal on detector. Detailed study of such influences was undertaken for each of the measured lines. To exclude any systematic error, each line was measured many times for different pressures (2–5 mTorr), and for different power and different line position on the baseline. This approach shows that, in our case, the typical scattering of the OCS line center, due to its different position on the base line, is about 0.5–1.5 kHz just exceeding the line center uncertainties obtained by individual line profile analysis. The half width of the Lamb-dip signal was about 15–30 kHz (HWHM) at a pressure of 2–3 mTorr, and this

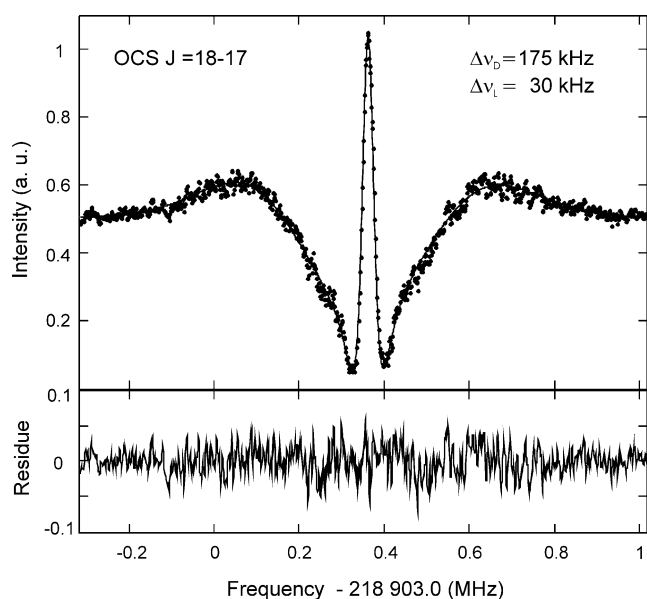


Fig. 1. Record of the OCS $J = 18 \leftarrow 17$ line, frequency modulation, and $2f$ detection was used. The observed values are denoted by points, the line represents the fit to Doppler profile with Lorentz shape dip; bottom trace is the residuum of the fit. The line center is 218903.3555(8) MHz; pressure in the cell was $P = 4.4$ mTorr at 301 K.

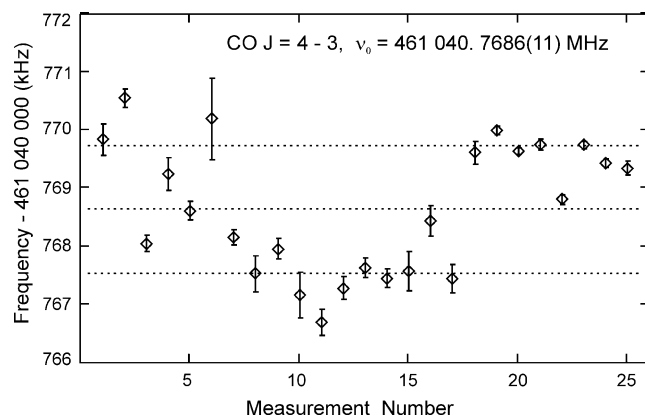


Fig. 2. The values of CO $J = 4 \leftarrow 3$ line centers measured at different experimental conditions. The mean center frequency of 461040.7686 ± 0.0011 MHz is obtained after averaging. The center value and the values corresponding to ± 1 SD are shown by dot lines.

Table 1

The frequencies of the rotational $^{12}\text{C}^{16}\text{O}$ lines measured in this work and calculated in [17]^a

Transition $J + 1 \leftarrow J$	Frequency (MHz), this work	Frequency (MHz), calc. from Ref. [17]	Obs. – Calc. (kHz)
2–1	230538.0000(5) [Kiel]	230537.99996(11)	0.0
3–2	345795.9898(4) [Kiel]	345795.98985(16)	0.0
4–3	461040.7686(11) [Kiel]	461040.76798(21)	0.6
8–7	921799.700(30) [Kiel]	921799.7042(4)	–4
8–7	921799.706(11) [NNov]	921799.7042(4)	+2
9–8	1036912.397(26) [NNov]	1036912.3852(5)	+12

^a Ref. [Kiel] in 2nd column means that the measurements were performed by Lamb-dip technique with the Kiel spectrometer with exception of the 921-GHz line measured by conventional absorption technique; Ref. [NNov] is used for the data obtained with the RAD spectrometer at Nizhnii Novgorod.

Table 2
Observed and calculated frequencies of the rotational $^{16}\text{O}^{12}\text{C}^{32}\text{S}$ lines^{a,b}

Transition $J + 1 \leftarrow J$	Observed frequency (MHz)	Ref.	Calculated frequency (MHz)	Obs. – Calc. (kHz)
1–0	12162.979(1)	[8]	12162.97902(1)	0.0
2–1	24325.927(1)	[8,9]	24325.92681(2)	0.2
3–2	36488.8128(10)	[6]	36488.81214(3)	0.7
3–2	36488.8121(4)	[12]	36488.81214(3)	0.0
4–3	48651.6043(10)	[11]	48651.60375(4)	0.5
4–3	48651.603(1)	Kiel	48651.60375(4)	–0.8
5–4	60814.270(15)	[19]	60814.27043(5)	–0.4
6–5	72976.7794(10)	[11]	72976.78094(6)	–1.5
7–6	85139.1032(7)	Kiel	85139.10404(07)	–0.8
8–7	97301.20849(12)	[10]	97301.20850(8)	0.0
9–8	109463.063(5)	[7]	109463.06308(9)	–0.1
10–9	121624.638(5)	[7]	121624.63654(9)	1.5
11–10	133785.900(5)	[7]	133785.89764(10)	2.4
12–11	145946.812(2)	[11]	145946.81516(11)	–3.2
13–12	158107.360(5)	[7]	158107.35785(11)	2.2
14–13	170267.494(5)	[7]	170267.49446(12)	–0.5
15–14	182427.1956(20)	[11]	182427.19377(12)	1.8
16–15	194586.433(10)	[7]	194586.42453(12)	8.5
17–16	206745.1558(8)	Kiel	206745.15550(13)	0.3
18–17	218903.3565(20)	[11]	218903.35543(13)	1.1
18–17	218903.3555(8)	Kiel	218903.35543(13)	0.1
19–18	231060.9934(13)	Kiel	231060.99308(13)	0.3
20–19	243218.0364(14)	Kiel	243218.03720(13)	–0.8
21–20	255374.4558(13)	Kiel	255374.45656(13)	–0.8
22–21	267530.2190(14)	Kiel	267530.21990(13)	–0.9
23–22	279685.2958(21)	Kiel	279685.29597(14)	–0.2
24–23	291839.6532(10)	Kiel	291839.65352(14)	–0.3
25–24	303993.2617(11)	Kiel	303993.26130(14)	0.4
26–25	316146.0890(12)	Kiel	316146.08805(14)	0.9
27–26	328298.1025(10)	Kiel	328298.10253(14)	0.0
28–27	340449.2733(8)	Kiel	340449.27347(15)	–0.2
29–28	352599.5703(12)	Kiel	352599.56961(15)	0.7
30–29	364748.9586(13)	Kiel	364748.95970(16)	–1.1
31–30	376897.4129(7)	Kiel	376897.41247(17)	0.4
32–31	389044.8976(11)	Kiel	389044.89666(18)	0.9
33–32	401191.3811(13)	Kiel	401191.38101(20)	0.1
34–33	413336.8344(10)	Kiel	413336.83423(21)	0.2
35–34	425481.2254(8)	Kiel	425481.22507(23)	0.3
36–35	437624.5221(7)	Kiel	437624.52225(25)	–0.2
37–36	449766.6936(14)	Kiel	449766.69450(28)	–0.9
38–37	461907.7107(10)	Kiel	461907.71053(30)	0.2
39–38	474047.5375(20)	Kiel	474047.53908(32)	–1.6
40–39	486186.1479(23)	Kiel	486186.14885(35)	–1.0
41–40	—		498323.50857(38)	—
42–41	—		510459.58694(41)	—
43–42	—		522594.35267(44)	—
44–43	—		534727.77449(47)	—
45–44	—		546859.82108(51)	—
46–45	—		558990.46115(54)	—
47–46	—		571119.66340(57)	—
48–47	—		583247.39652(61)	—
49–48	—		595373.62922(64)	—
50–49	—		607498.33018(68)	—
51–50	—		619621.46808(72)	—
52–51	—		631743.01161(75)	—
53–52	—		643862.92945(79)	—
54–53	—		655981.19028(83)	—
55–54	—		668097.76277(87)	—
56–55	—		680212.61559(90)	—
57–56	—		692325.71740(94)	—
58–57	704437.052(60)	[20]	704437.03688(98)	15
59–58	716546.559(60)	[20]	716546.5427(10)	16
60–59	—		728654.2035(11)	—
61–60	—		740759.9879(11)	—

Table 2 (continued)

Transition $J + 1 \leftarrow J$	Observed frequency (MHz)	Ref.	Calculated frequency (MHz)	Obs. – Calc. (kHz)
62–61	—		752863.8645(11)	—
63–62	—		764965.8021(12)	—
64–63	—		777065.7693(12)	—
65–64	789163.801(200)	[21]	789163.7346(13)	66
66–65	801259.782(200)	[20]	801259.6668(13)	115
67–66	813353.706(200)	[20]	813353.5344(14)	172
68–67	—		825445.3062(14)	—
69–68	—		837534.9506(15)	—
70–69	—		849622.4363(15)	—
71–70	—		861707.7319(16)	—
72–71	—		873790.8061(17)	—
73–72	—		885871.6274(17)	—
74–73	897950.171(7)	NNov	897950.1644(18)	7
75–74	910026.384(11)	NNov	910026.3858(19)	–2
76–75	922100.248(16)	Kiel	922100.2600(20)	–12
76–75	922100.238(11)	NNov	922100.2600(20)	–22
77–76	934171.756(13)	Kiel	934171.7558(22)	0
77–76	934171.769(10)	NNov	934171.7558(22)	13
78–77	946240.830(11)	NNov	946240.8416(23)	–12
79–78	958307.437(28)	NNov	958307.4860(24)	–49
80–79	—		970371.6577(26)	—
81–80	—		982433.3251(28)	—
82–81	—		994492.4568(29)	—
83–82	—		1006549.0215(31)	—
84–83	—		1018602.9875(34)	—
85–84	1030654.359(27)	NNov	1030654.3235(36)	35
86–85	1042702.991(16)	NNov	1042702.9980(39)	–7
87–86	1054748.975(16)	NNov	1054748.9795(41)	–5
88–87	1066792.231(10)	NNov	1066792.2366(44)	–6
89–88	1078832.802(23)	NNov	1078832.7378(47)	64
90–89	1090870.459(29)	NNov	1090870.4516(51)	7
91–90	1102905.314(200)	[21]	1102905.3464(54)	–32
92–91	—		1114937.3909(58)	—
93–92	1126966.568(200)	[21]	1126966.5534(63)	15

^a Ref. [Kiel] in 3rd column means that the measurements were performed by Lamb-dip technique with the spectrometer at Kiel with the exception of the 922- and 934-GHz lines which were measured by conventional absorption technique; Ref. [NNov] is used for the data obtained with RAD spectrometer at Nizhny Novgorod.

^b Uncertainties given in parentheses are in units of the last digit quoted; this work values are 1 SD obtained after averaging of many line records at different conditions.

is about one order of magnitude lower than the Doppler width.

Additional test measurements of rotational CO lines, known very precisely, have been performed to check our accuracy. In Table 1, values of our CO frequencies and precisely measured lines in [17] show a good consistency. Similarly to OCS, measurements of CO lines were done at different baseline conditions to determine the final transition frequency and one standard deviations was taken as the uncertainty affecting the mean frequency. Typical example of baseline influence on the line center of CO $J = 4 \leftarrow 3$ transition is shown in Fig. 2.

Altogether 26 rotational OCS transitions have been measured with an accuracy of about one kHz by Lamb-dip technique. Twelve OCS transitions in THz frequency range were measured with an accuracy ≤ 30 kHz. All newly obtained and previously measured OCS frequencies are listed in 2nd column of Table 2.

Among the previous line measurements, we have included in our fit all precise molecular beam and some of Lamb-dip data. So far the frequency uncertainties of Winton and Gordy [7] are several times lower in comparison with our accuracies, theirs data above 200 GHz have been discarded. Those measurements of [7] below 200 GHz have been included in the fit when no data from Dubrulle et al. [11] were available.

The calculated frequencies based on our fit are given in 4th column. Fifth column lists the Obs. – Calc. residuals and it is seen that nearly for all our measurements below 500 GHz the Obs. – Calc. parameter is within 1 kHz. The estimated rotational constants B_0 is more than 2 times and D_0 is more than one order of magnitude accurate in comparison with the previous result [11] as it is shown in Table 3. This is about one to two orders of magnitude more accurate compared with the traditional Doppler spectroscopy (see, for example, recent work on rare OCS isotopomers [18]).

Table 3

Rotational constants of $^{16}\text{O}^{12}\text{C}^{32}\text{S}$ obtained from the fit of the line center frequencies listed in Table 2

Constant	This work	Ref. [11]
B_0 (MHz)	6081.4921150(52)	6081.492106(12)
D_0 (kHz)	1.3014274(32)	1.301367(50)
H_0 (mHz)	−0.08938(33)	—

The OCS rotational lines can be considered as a good secondary standard for precise laboratory measurements of frequencies so far as the uncertainties for all calculated rotational $^{16}\text{O}^{12}\text{C}^{32}\text{S}$ transitions in the ground vibrational state below 500 GHz do not exceed 1 kHz and no significant pressure shift was found at room temperature [12].

Acknowledgments

The present work was supported by DFG project 436 RUS 113/750/0-1 and in part by the RFBR-DFG No. 04-02-04003, RFBR No. 03-02-16125, No.05-07-90196-B, and No. 03-02-16307. To all these sources of support the authors express their deep gratitude. Additionally, we want to thank the central workshop of the Technische Fakultät (Kiel) for manufacturing necessary millimeter- and submillimeter-wave elements.

References

- [1] G. Cazzoli, C. Puzzarini, A. Lapinov, *Astrophys. J.* 592 (2003) L95–L98.

- [2] G. Cazzoli, C. Puzzarini, A. Lapinov, *Astrophys. J.* 611 (2004) 615–620.
- [3] J.M.L.J. Reinartz, A. Dymanus, *Chem. Phys. Lett.* 24 (1974) 346–351.
- [4] R. Mauersberger, C. Henkel, Y.-N. Chin, *Astron. Astrophys.* 294 (1995) 23–32.
- [5] S. Martín, J. Martín-Pintado, R. Mauersberger, C. Henkel, S. García-Burillo, *Astrophys. J.* 620 (2005) 210–216.
- [6] C.C. Costain, *Can. J. Phys.* 47 (1969) 2431–2433.
- [7] R.S. Winton, W. Gordy, *Phys. Lett.* 32A (1970) 219–220.
- [8] S.G. Kukolich, D.E. Oates, J.H.S. Wang, *J. Chem. Phys.* 61 (1974) 4686–4689.
- [9] J.H.S. Wang, D.E. Oates, A. Ben-Reuven, S.G. Kukolich, *J. Chem. Phys.* 59 (1973) 5268–5276.
- [10] F.A. van Dijk, A. Dymanus, *Chem. Phys.* 6 (1974) 474–478.
- [11] A. Dubrulle, J. Demaison, J. Burie, D. Boucher, *Z. Naturforsch.* 35a (1980) 471–474.
- [12] J.P.M. De Vreede, M.P.W. Gillis, H.A. Dijkerman, *J. Mol. Spectrosc.* 128 (1988) 509–520.
- [13] A. Huckauf, A. Guarnieri, *J. Mol. Spectrosc.* 213 (2002) 79–85, <http://hf.tf.uni-kiel.de/Research/MoleculeSpectroscopy/>.
- [14] G.Yu. Golubiatnikov, A.F. Krupnov, *J. Mol. Spectrosc.* 217 (2003) 282–287, <http://www.appl.sci-nnov.ru/mwl/index.htm>.
- [15] G. Cazzoli, L. Dore, *J. Mol. Spectrosc.* 141 (1990) 49–58.
- [16] G. Cazzoli, L. Dore, *J. Mol. Spectrosc.* 143 (1990) 231–236.
- [17] G. Winnewisser, S.P. Belov, Th. Klaus, R. Schieder, *J. Mol. Spectrosc.* 184 (1997) 468–472.
- [18] K. Kubo, T. Furuya, S. Saito, *J. Mol. Spectrosc.* 222 (2003) 255–262.
- [19] N.W. Larsen, B.P. Winnewisser, *Z. Naturforsch.* 29a (1974) 1213–1215.
- [20] P. Helminger, F.C. De Lucia, W. Gordy, *Phys. Rev. Lett.* 25 (1970) 1397–1399.
- [21] M.D. Vanek, D.A. Jennings, J.S. Wells, A.G. Maki, *J. Mol. Spectrosc.* 138 (1989) 79–83.